Food Chemistry: X 23 (2024) 101510

Contents lists available at ScienceDirect

Food Chemistry: X

journal homepage: www.sciencedirect.com/journal/food-chemistry-x

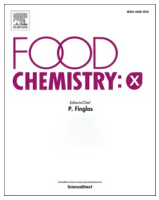

# Preparation and characterization of tea tree essential oil microcapsule-coated packaging paper with bacteriostatic effect

Lin Zhu [a,b], Yijun Liu [a,b], Jiameng Liu [a,b], Xunxia Qiu [a,b], Lijing Lin [a,b,*]

[a] Key Laboratory of Tropical Crop Products Processing of Ministry of Agriculture and Rural Affairs, Agricultural Products Processing Research Institute, Chinese Academy of Tropical Agricultural Sciences, Zhanjiang, Guangdong 524001, China
[b] Hainan Key Laboratory of Storage and Processing of Fruits and Vegetables, Zhanjiang, Guangdong 524001, China

ARTICLE INFO

*Keywords:*
Antibacterial
Coated Kraft paper
Pullulan
Structural characterization
Tea tree essential oil microcapsule

ABSTRACT

We prepared tea tree essential oil microcapsules, and the microcapsules and pullulan were coated on kraft paper to prepare an antibacterial paper. The antibacterial activity, structural characterization, and thermal stability of the prepared microcapsules and packaging paper were then tested. We found that the retention rate of microcapsules reached 87.1% after a 70 min of high-temperature treatment. The minimum inhibitory concentrations of microcapsules to *S. aureus* and *E. coli* were 112 mg/mL and 224 mg/mL, and the bacteriostatic zones of the packaging paper to *E. coli* and *S. aureus* were 17.49 mm and 22.75 mm, respectively. The prepared microcapsules were irregular. The paper coating was formed via hydrogen bonding, which filled the pores of paper fibers. When compared with the base paper, the roughness of the paper was reduced to 7.16 nm (Rq) and 5.61 nm (Ra), and no thermal decomposition occurred at <288 °C, which together implies a good application prospect.

## 1. Introduction

Owing to continuous improvements in living standards and health awareness, people are gradually realizing the hidden dangers of conventional chemical preservation technologies. Hence, there has been an increasing interest in the pursuit of safe, environmentally friendly, and green natural preservation methods, of which plant essential oils have gained the research focus in recent years. Tea tree essential oil (TTO) is a light-yellow oil obtained from the branches and leaves of *Melaleuc alternifolia* of *Myrtaceae* via steam distillation(Hu et al., 2023). Because of its high efficiency and nontoxicity, TTO can effectively inhibit various bacteria and fungi, prolong the storage period of fruits and vegetables, and may even replace chemical fungicides as a new preservative(Cao et al., 2021). However, owing to its strong smell, volatility, and instability in practical application, it has to be applied for the postharvest preservation of fruits and vegetables using emulsification, microencapsulation, and other such methods.

Microcapsules embed substances in wall materials and release them in a specific environment The substance captured inside a microcapsule is called the core material and is often volatile and environmentally sensitive (Huang et al., 2024), the encapsulating helps avoid the loss of nutritional value, discoloration, and taste deterioration. Cyclodextrin (CD), including its derivatives, is usually used as the wall material for encapsulating active ingredients. The CD is a cyclic oligosaccharide that is easily available and cheap, but limited in its application owing to its poor water solubility (Wang, Yan, Yan, & Wang, 2023). Therefore, different functional groups have been introduced to form its derivatives. For example, hydroxypropyl-β-cyclodextrin (HP-β-CD) is the etherification product of β-cyclodextrin. By introducing a hydroxypropyl group into β-cyclodextrin, the intramolecular cyclic hydrogen bond is destroyed, and the water solubility is improved. Meanwhile, the lipophilic cavity of cyclodextrin is maintained, which offers the advantages of strong inclusion ability, less irritation, and safety (Du, Xu, Wang, Yuan, & Hu, 2009). Microcapsules formed by cyclodextrin wall materials can improve the thermal stability (Emadzadeh, Ghorani, Naji-Tabasi, Charpashlo, & Molaveisi, 2021) and water solubility (Huang et al., 2024) of the entrapped essential oils. For example, Hu et al. (2024) prepared microcapsules of emulsified cinnamon essential oil (CEO) with HP-β-CD/lauroyl arginine ethyl ester complex, compounded with maltodextrin (MD), by spray drying method, and it delayed the volatilization of the CEO. Clove essential oil and hydroxypropyl-β-cyclodextrin formed an inclusion complex, and the water solubility of CEO was obviously improved by complexation. Moreover, Ying et al. (2024) prepared oregano essential oil (OEO)/β-CD successfully coated OEO,

* Corresponding author at: Key Laboratory of Tropical Crop Products Processing of Ministry of Agriculture and Rural Affairs, Agricultural Products Processing Research Institute, Chinese Academy of Tropical Agricultural Sciences, Zhanjiang, Guangdong 524001, China
*E-mail address:* linlijing0763@163.com (L. Lin).

https://doi.org/10.1016/j.fochx.2024.101510
Received 30 April 2024; Received in revised form 23 May 2024; Accepted 24 May 2024
Available online 28 May 2024

which effectively improved its thermal stability. In addition, Cao et al. (2021) employed the coprecipitation method to prepare a large cyclodextrin/TTO complex. The thermal stability and water solubility of TTO were improved, and the solubility of the complex was increased by 329 times. However, after the fruits and vegetables were treated using these methods, the unique smell of TTO easily penetrated their edible parts, which seriously affected the edible quality. Moreover, TTO in the epidermis of fruits and vegetables volatilizes easily and therefore does not exert a long-term antiseptic effect. Some researchers emulsified plant essential oil, mixed it with other surface-sizing agents, and directly coated it on the surface of a paper base to prepare paper-based materials.

As the most representative sustainable natural green material, paper-based materials have been applied extensively in various fields of life and production(Ham-Pichavant, Sèbe, Pardon, & Coma, 2005). Novel functional paper-based materials offer immense advantages in terms of physical properties, energy saving and environmental protection, and mechanical operation performance. These materials have attracted the attention of the research community for fruit and vegetable preservation. The new functional paper-based food packaging mainly includes waterproof functional paper packaging(Kunam & Gaikwad, 2023), thermal food packaging paper, food packaging preservative paper (Xia et al., 2024), and edible packaging paper. Of these, food packaging preservative paper can inhibit food spoilage simply via the packaging paper without the use of preservatives and maintain food freshness by absorbing the water on the food surface or even inside it. Khwaldia (2010) studied the potential of composite materials formed from sodium caseinate-coated paper in the packaging field and found that the water vapor barrier and mechanical properties of such composite materials were significantly improved compared with those of the original paper. In another study(Chu, Popovich, & Wang, 2023), the influence of zein on the water vapor and oxygen barrier properties of paper-based materials was examined, which revealed that these properties of zein paper-based composites were improved under coating conditions.

Food decay and deterioration can result in economic losses and environmental problems, among which food waste and human infection due to food decay and deterioration induced by microorganisms occupy an inestimable position. Among human pathogens, *Staphylococcus aureus* and *Escherichia coli* are the main infection-causing pathogens (Jayakumar et al., 2022). At the same time, *E. coli* is a gram-negative bacterium, and *S. aureus* is a gram-positive bacterium, which was applied to the antibacterial test of materials. Gao et al. (2024) prepared chitosan/carboxymethyl dextran/polyvinyl alcohol/nano-particles-coated citral composite film. Taking *S. aureus* and *E. coli* as typical model bacteria, it was found that the antibacterial rates against *S. aureus* and *E. coli* were 97.5% and 96.2%, respectively, displaying a strong antibacterial performance. Cellulose nanofiber /Ta4C3T x packaging was found to exert a certain antibacterial effect, with the inhibition rate for *E. coli* being 67% and that for *S. aureus* being 59%(Wang et al., 2024).

Ordinary paper-based materials cannot resolve the problems associated with the easily oxidizable and volatilizable nature of TTO when applied to paper-based materials. Hence, in this study, TTO microcapsules were prepared as antibacterial agents and their thermal stability was explored. Their structural characteristics were determined using X-ray diffraction (XRD), Fourier-transformed infrared (FT-IR) spectroscopy, and scanning electron microscopy (SEM). A new type of bioactive paper-based material with good antibacterial properties was prepared by coating TTO microcapsules on the surface of paper-based materials by using the surface-sizing method. The material was studied using the techniques of XRD, FT-IR, SEM, and atomic force microscopy (AFM). To provide basic data and theoretical support for postharvest storage, transportation, and preservation of fruits and vegetables, the bacteriostatic mechanism was systematically studied using bacteriostatic circle, bacteriostatic rate, and SEM.

## 2. Materials and methods

### 2.1. Materials and reagents

Hydroxypropyl-β-cyclodextrin (HP-β-CD) was purchased from Shanghai Yuanye Biotechnology Co., Ltd. (Shanghai, China); TTO was prepared in the laboratory (Zhanjiang, China); anhydrous ethanol and glutaraldehyde stationary solution (2.5%) were purchased from Sinopharm Chemical Reagents Co., Ltd. (Shanghai, China); pullulan was purchased from Aladdin (Shanghai, China); LB broth, LB agar, nutrient broth, nutrient solid, *E. coli* CMCC(B)44,102, and *S. aureus* CMCC(B) 26,003 were all purchased from Guangdong Huankai Microbial Technology Co., Ltd. (Guangzhou, China), and kraft paper was purchased from Foshan Guangshibo Office Supplies Co., Ltd. (Foshan, China).

### 2.2. Preparation of TTO microcapsules

A 20% HP-β-CD solution was prepared by dissolving HP-β-CD in 1% ethanol solution. Then, TTO (1:6, w essential oil /w HP-β-CD, based on dry weight) was slowly added to the warm HP-β-CD solution, and the mixture (Miou Instrument TP-350E+, China) was stirred at 50 °C for 3 h. The final solution was maintained at 4 °C overnight and vacuum filtered to recover the precipitate, followed by vacuum freeze-drying (Christ Alpha1–4 LSC PLUS, Germany) for 48 h; the final TTO microcapsules were stored in a sealed bottle at 25 °C and the control (without TTO) HP-β-CD microcapsules were prepared in triplicate(Kong, Abe, Masuo, & Enomae, 2023).

### 2.3. Effect of high temperature on the retention rate of TTO:HP-β-CD microencapsulated TTO

Weighing bottle containing 0.3 g of TTO and TTO microcapsules was placed in different ovens(Shanghai-Heng Scientific Instrument DHG-9140 A, China) at 100 °C, and the mass at the 0, 10, 20, 30, 40, 50, 60, and 70 min of slow release was determined, followed by the calculation of the retention rate (Y′) of TTO using the following formula(Andrade, 2023):

$$Y' = m_t/m_0 \times 100\% \quad (1)$$

where, $m_0$ represents the initial mass of the sample, g; $m_t$ represents the sample mass after the slow release t time, g.

### 2.4. Bacteriostasis experiment of microcapsules

#### 2.4.1. Minimum inhibitory concentration (MIC)

The MIC of microcapsules was tested by using the double dilution method. First, 224, 112, 56, 28, 14, 7, and 3.5 mg/mL of the TTO microcapsule suspensions were prepared and mixed in the liquid culture medium of nutrient broth in a 1:1 volume ratio (total volume, 5 mL). For the experimental group, 0.5 mL of the Turbidite suspension with a bacterial content of approximately 0.5 was inoculated into the liquid culture medium test tube containing microcapsules. The control group was composed of a culture medium of pure bacterial liquid (2.5 mL sterilized water and 2.5 mL liquid culture medium). The experimental and control group test tubes were placed in an incubator (Shanghai Lichen Bangxi HH-6, China) at 37 °C for 24 h, and the growth of the bacteria in the test tube (turbidity) was examined with the naked eye. The minimum concentration of the microcapsule suspension without turbidity was MIC (Kızılyıldırım et al., 2024).

### 2.5. Characterization of microcapsules

#### 2.5.1. Surface morphology of microcapsules

The surface structures of HP-β-CD, TTO microcapsules, and HP-β-CD microcapsules without TTO were observed by SEM (Hitachi SU1510,

Japan) after spraying with gold(Li et al., 2022).

#### 2.5.2. Infrared spectrum of microcapsules

HP-β-CD, TTO, and TTO microcapsules were tableted by the potassium bromide (KBr) method. Briefly, KBr (solid dispersant, 150–200 mg) was added to 1–2 mg of the samples, mixed evenly, ground for 2 min, and tableted by using a tableting machine followed by determination by infrared spectroscopy (IN10, Thermo Fisher Scientific, Germany) in the range of 500–5000 $cm^{-1}$(Ahmad, Qureshi, Maqsood, Gani, & Masoodi, 2017).

#### 2.5.3. X-ray diffraction of microcapsules

X-ray diffraction (Bruker D8 Venture, Germany) was used to analyze HP-β-CD, HP-β-CD microcapsules, and TTO microcapsules under the following test conditions: scanning range (2θ = 5°- 80°) and scanning speed (10°/min)(Lai et al., 2022).

### 2.6. Preparation of antibacterial food packaging paper

#### 2.6.1. Preparation of microencapsulated composite coatings of TTO

Pullulan (2 g) was fully dissolved in 50 mL of distilled water to obtain a pullulan solution for use as a coating adhesive, which was evenly stirred at 50 °C. TTO microcapsules were then added into the pullulan solution at a mass ratio of 1:28 and stirred at 500 rpm for 20 min to obtain a microcapsule composite coating with antibacterial properties (Inthamat, Karbowiak, Tongdeesoontorn, & Siripatrawan, 2024).

#### 2.6.2. Preparation and characterization of antibacterial food packaging paper

A simple coating board (WD2608, Dalai, Dongguan) was used to coat the composite coating of TTO microcapsules, and the paper was dried at room temperature (23 ± 2 °C) for 24 h, with the basis weight of 100 g/$m^2$ and the coating amount of 25.7 g/$dm^2$. The paper was termed PP/TTO paper. In addition, the base paper and pullulan solution-coated paper (PP paper) served as controls. In order to normalize the moisture content of the papers, all samples were balanced in a constant temperature and humidity chamber at 25 °C under 50% RH (Inthamat et al., 2024).

### 2.7. Antibacterial food packaging paper

#### 2.7.1. Bacteriostatic circle of antibacterial food packaging paper

The suspensions of *S. aureus* and *E. coli* (1 × $10^6$ CFU/mL) were prepared in LB liquid culture medium, diluted with physiological saline to $10^6$ CFU/mL bacterial suspension, and shaken evenly. Then, 200 μL of the suspension was evenly coated on the LB solid medium prepared for both groups, the paper of the experimental group and the control group (by ultraviolet for 2 h) was attached to the center of the plate containing bacteria and cultured for 24 h in an incubator (Ningbo Jiangnan Instrument HWM-358, China) at 37 °C. Three parallel samples were set for each group, and the diameter of the bacteriostatic circle was measured (Lian, Cao, Jiang, & Rogachev, 2021).

#### 2.7.2. Bacteriostatic rate of antibacterial food packaging paper

The bacteriostatic rate was tested by the OD method. The samples were prepared into 15 mm discs with a punch and placed in an ultra-clean table(Suzhou Purification SW-CJ-2FD, China) for ultraviolet sterilization for 30 min. In the experiment, $10^6$ CFU/mL of the bacterial suspension was inoculated into the liquid culture medium, and the paper was placed in the liquid culture medium for 12 h at 37 °C, followed by absorbance measurement at 600 nm(Zhu, Luo, Shi, & Chen, 2023).

$$\text{Bacteriostasis rate} = (OD600_1 - OD600_2/OD600_1 \times 100\% \quad (2)$$

$OD600_1$ = OD600 without paper medium, and $OD600_2$ = OD600 with paper.

#### 2.7.3. Observation of the antibacterial ultrastructure of antibacterial food packaging paper

The antibacterial food packaging paper was tested by SEM (Hitachi SU1510, Japan), and a 15-mm disc was prepared with a punch, which was placed in a super clean table for ultraviolet sterilization for 30 min. In the experiment, $10^6$ CFU/mL bacterial liquid was inoculated into the liquid culture medium, and the antibacterial food packaging paper was placed in the liquid culture medium and cultured for 12 h at 37 °C. Then, the antibacterial food packaging paper was removed, centrifuged at 25 °C and 8000 rmp for 3 min, and the bacterial precipitate was retained. It was then fixed with 2.5% glutaraldehyde for 4 h, rinsed thrice with PBS, and finally dehydrated with different gradient ethanol for 5 min and 50% tert-butyl alcohol(Zhu et al., 2023).

### 2.8. Characterization and measurement of antibacterial packaging paper

#### 2.8.1. Scanning electron microscope

SEM (Hitachi SU1510, Japan) was used to analyze the surface and cross-section morphology of antibacterial packaging paper, and the cross-section was frozen and broken by liquid nitrogen. The antibacterial packaging paper was sprayed with gold and observed under a certain magnification(Karami-Eshkaftaki, Saei-Dehkordi, Albadi, Moradi, & Saei-Dehkordi, 2024).

#### 2.8.2. X-ray diffraction analysis

The antibacterial packaging paper was placed on an X-ray diffractometer (Bruker D8 Venture) for scanning under the following test conditions: scanning range (2θ = 5°–80°) and scanning speed (10°/min) (Lai et al., 2022).

#### 2.8.3. Infrared spectrum of microcapsules

The antibacterial packaging paper was tableted by the KBr method and determined by infrared spectroscopy (IN10, Thermo Fisher Scientific) in the range of 500–5000 $cm^{-1}$(Karami-Eshkaftaki et al., 2024).

#### 2.8.4. Atomic force microscope

The surface characteristics and roughness of antibacterial food packaging paper were analyzed by atomic force microscope (BD NANOSURF C300, USA), and the images were captured in the tapping mode. The paper was placed on the sample table and scanned over an area of 10 um × 10 um. The three-dimensional structure and roughness of the antibacterial food packaging paper were quantitatively evaluated by using a gwyddion software(Pinto et al., 2023).

#### 2.8.5. Thermogravimetric analyzer

A thermogravimetric analyzer (TA Discovery TGA 550, USA) was used to analyze the thermal stability of antibacterial food packaging paper at the test temperature of 30–600 °C. The heating rate was 10.00 °C/min, and the temperature was maintained for 1 min(Zhu et al., 2023).

### 2.9. Data processing and analysis

MS Excel was used to analyze the measured data, Origin 2021 software was used for drawing. The data were statistically analyzed by SPSS22.0, expressed as the mean value and standard deviation, and tested by independent sample *t*-test.

## 3. Results and discussion

### 3.1. Effect of high temperature on the retention rate of TTO and TTO:HP-β-CD microcapsules

The retention curve of TTO and TTO microcapsules at 100 °C is presented in Fig. 1A. As shown in the figure, as the sustained release time extended, the retention rate of TTO in the microcapsules gradually

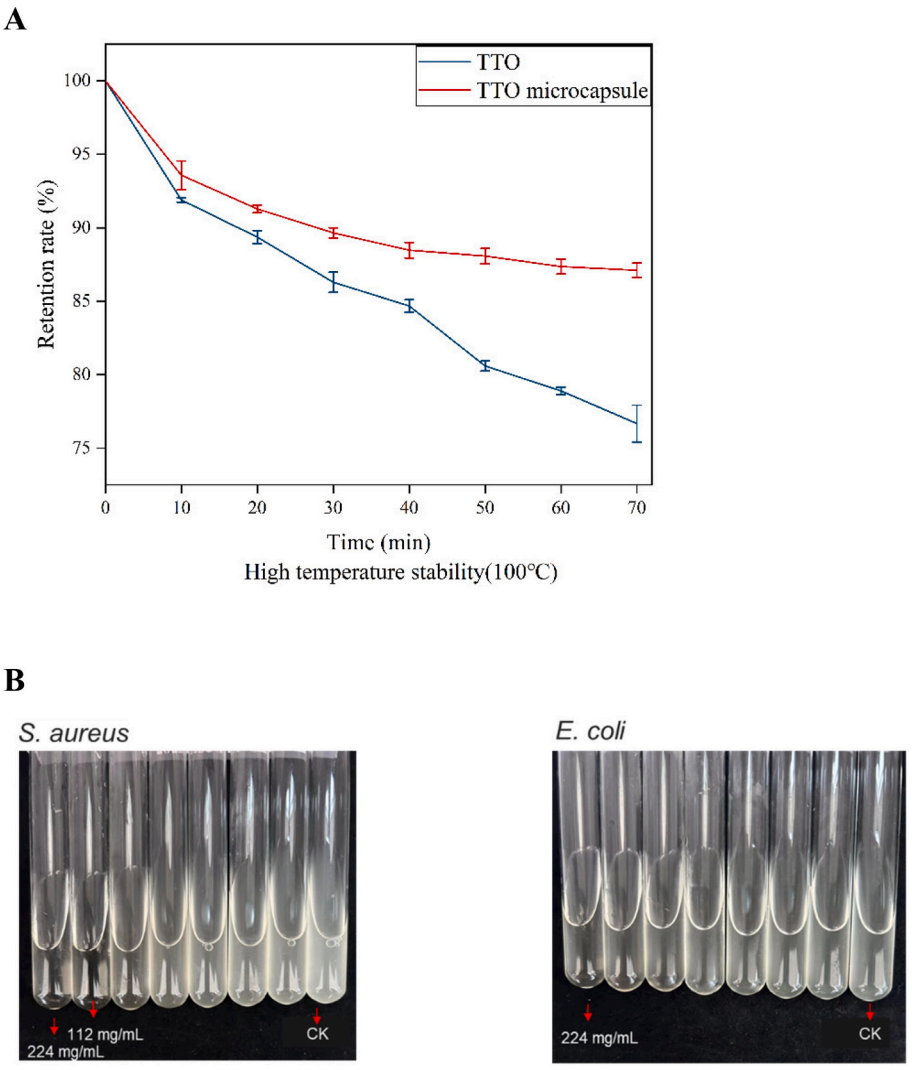


**Fig. 1.** Effect of high temperature (100 °C) on the retention rate of tea tree essential oil and TTO:HP-β-CD microcapsules (A). Minimum inhibitory concentration (MIC) of TTO microcapsules (B).

decreased. The release rate of TTO in the microcapsules was faster when it was released for 0–10 min, which may be due to the rapid volatilization of a small amount of TTO on the surface of HP-β-CD(Hu et al., 2024). After 40 min of sustained release, the volatilization of TTO in the microcapsules was slow, and the sustained release effect was good. As shown in Fig. 1A, after the sample was treated at 100 °C for 70 min, the retention rate of TTO microcapsules reached 87.1%, while the retention rate of TTO was only 76.7%, which was higher than that of untreated TTO; as such the retention effect was good and the high-temperature stability was improved.

### 3.2. Minimum inhibitory concentration (MIC) of the microcapsules

The experimental results of the MIC concentration of TTO microcapsules against *S. aureus* and *E. coli* are depicted in Fig. 1B and Table 1.

**Table 1**
Antibacterial activity of tea tree essential oil microcapsules against *Staphylococcus aureus* and *Escherichia coli*.

| Sample | MIC (mg/mL) | |
|---|---|---|
| | *S. aureus* | *E. coli* |
| TTO: HP-β-CD microcapsules | 112 mg/mL | 224 mg/mL |

As presented in the table, the TTO microcapsules inhibited the growth and reproduction of the two tested bacteria to varying degrees. As inferred from Fig. 1B, the MIC of the microcapsules for *S. aureus* was 112 mg/mL and that for *E. coli* was 224 mg/mL. The cell wall structure of gram-positive and gram-negative microorganisms is different, which leads to variations in the degree of reaction to the essential oil. Gram-positive bacteria have a thick peptidoglycan layer, which promotes the transport of lipophilic molecules, such as essential oil, across the membrane. However, gram-negative bacteria have a double-layered membrane, and the outer layer contains a lipopolysaccharide layer, which poses difficulties in the transport of essential oil across the membrane(Medeleanu et al., 2023). Therefore, the antibacterial effect of TTO microcapsules on *S. aureus* was more prominent than that on *E. coli*.

### 3.3. SEM of the microcapsules

Morphological examination is a qualitative technique to observe the surface morphology of raw materials or prepared samples. The SEM images of HP-β-CD, HP-β-CD microcapsules, and TTO/HP-β-CD microcapsules are shown in Fig. 2A. The original untreated HP-β-CD was spherical, and the hollow sphere was large and uneven in size, with a large inner cavity and a thick wall. Moreover, the spherical wall had developed pores. The typical form of HP-β-CD was amorphous spherical

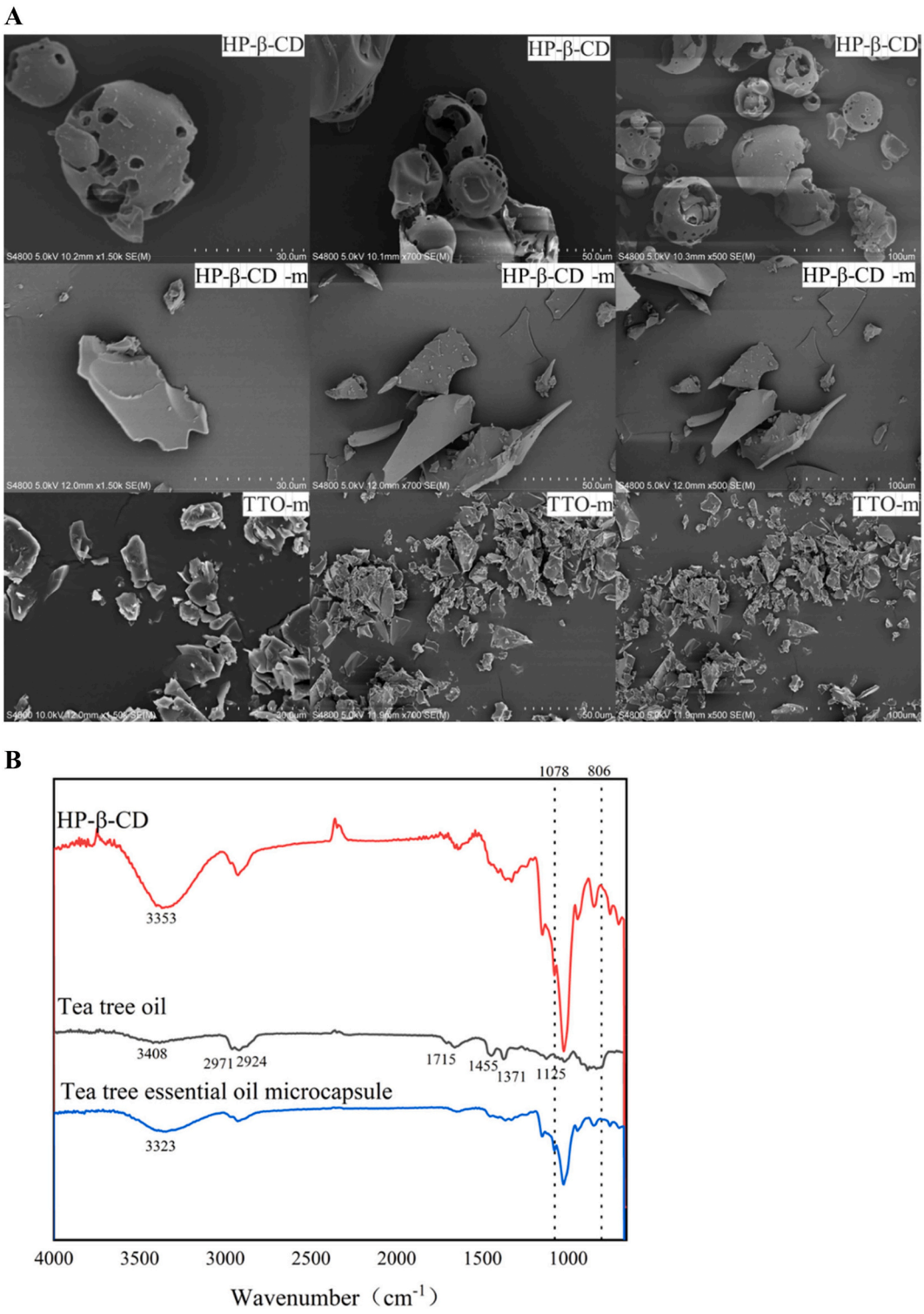


**Fig. 2.** Scanning electron microscopy (SEM) revealed that HP-β-CD was untreated hydroxypropyl-β-cyclodextrin, HP-β-CD-m is HP-β-CD microcapsule, TTO-m is a microcapsule of TTO. The magnifications of HP-β-CD, HP-β-CD-m, and TTO-m are 1500 times, 700 times, and 500 times, respectively. (A). Infrared spectrogram of microcapsules (B). The X-ray diffraction pattern of microcapsules (C).

particles with a cavity structure(Qiang, Wei, Huang, Chi, & Fu, 2024). During the reaction process, the morphology of HP-β-CD may change (Munhuweyi, Caleb, van Reenen, & Opara, 2018), resulting in the development of morphological differences before and after the HP-β-CD reaction. After the formation of microcapsules, HP-β-CD changed from a spherical hollow to an irregular homogeneous block or plate, forming crystals of different sizes with obvious small particles on the surface. After the microencapsulation of TTO, the TTO microcapsules were much smaller in rhombic size and tended to aggregate compared with the HP-β-CD microcapsules (without TTO). The inclusion compound exhibited an irregular block structure with a significantly smaller size and rhombic crystal (Wen et al., 2016), which agrees with the findings of previous

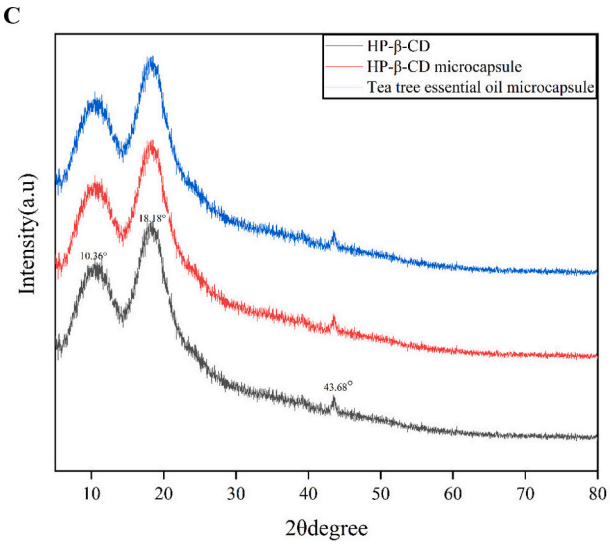


**Fig. 2.** (*continued*).

studies(Guan et al., 2024; Qiang et al., 2024; Wen et al., 2016; Yang et al., 2022). This remarkable change in particle morphology could be attributed to the interaction between TTO and HP-β-CD and may also be linked to the water loss during the TTO/HP-β-CD reaction(Qiang et al., 2024).

### 3.4. Infrared spectrum of the microcapsules

Fig. 2B shows the FT-IR spectra of HP-β-CD, TTO, and TTO microcapsules. TTO exhibited O—H tensile vibration at 3408 $cm^{-1}$, 2971 $cm^{-1}$, and 2924 $cm^{-1}$ and symmetric and asymmetric tensile vibration at $–CH_3$ and $-CH_2-$. The weak absorption peak at 1800–1600 $cm^{-1}$ was terpene C═C, and the absorption peaks at 1455 $cm^{-1}$ and 1371 $cm^{-1}$ were aromatic C═C, $-CH_3$, and $-CH_2-$ vibration(Cui, Bai, & Lin, 2018). The absorption peak at 1125 $cm^{-1}$ was the tensile vibration of the C—O bond in terpineol, and the peak at 1078 $cm^{-1}$ was the symmetric tensile vibration of 1,8-cineole C-O–C in TTO. At 860 and 800 $cm^{-1}$, the peak could be attributed to the para-position substitution of benzene in TTO (Kong et al., 2023). The main absorption bands of HP-β-CD were observed at 3353, 2924, 1650, 1157, and 1029 $cm^{-1}$, which corresponded to the symmetric and asymmetric tensile vibration of O—H, the tensile vibration of C—H, the bending of H-O-H, the tensile vibration of C—O, and the symmetric and asymmetric tensile vibration of C-O-C, respectively. It is worth noting that the spectrum of TTO microcapsules was predominantly HP-β-CD, and the peak of TTO at 2971–2924 $cm^{-1}$ was weakened in the spectrum of TTO microcapsules, and the peak intensity at 1371 $cm^{-1}$ was partially reduced. Furthermore, the aromatic C═C peak was almost completely hidden by HP-β-CD, which is consistent with the observation of (Wen et al., 2016)and may be related to the successful embedding of TTO. In addition, the O—H absorption peak of TTO microcapsules shifted to a lower frequency (redshift) relative to HP-β-CD, which signified the interaction of the bioactive compound TTO with HP-β-CD via hydrogen bonds (Munhuweyi et al., 2018). These observations confirm that the microencapsulation was successful.

### 3.5. X-ray diffraction of the microcapsules

The physical states of HP-β-CD, HP-β-CD microcapsules, and TTO microcapsules were analyzed using XRD. Fig. 2C shows that the XRD patterns of TTO microcapsules and HP-β-CD microcapsules were consistent with those of HP-β-CD itself. HP-β-CD microcapsules and TTO microcapsules were at 10.36°, 18.18°, and 43.68°. The characteristic peak of HP-β-CD itself was observed(Hu et al., 2023), indicating that TTO was completely embedded in HP-β-CD and encapsulated by it in the form of an inclusion compound, which agreed with the results of FT-IR. In other words, the diffraction pattern of the microcapsules was the superposition of the peaks on the HP-β-CD diffraction pattern, and the diffraction angles of HP-β-CD itself in TTO microcapsules and HP-β-CD microcapsules have not changed obviously. This finding implies that when TTO forms an inclusion complex with HP-β-CD, its crystal configuration does not change significantly and it has no new phase compared with HP-β-CD itself, which is consistent with past reports (Sun, Zhu, Liu, Wang, & Wang, 2022), the peak of fucoxanthin disappears, and the inclusion compound only showed diffraction peaks of 2-HP-β-CD at 2θ ~ 10° and 18°.

### 3.6. Antibacterial food packaging paper

#### 3.6.1. Bacteriostatic circle and bacteriostatic rate of antibacterial food packaging paper

The diameter of the bacteriostatic ring represents the bacteriostatic ability to a certain extent, and the experimental results of a bacteriostatic ring of antibacterial food packaging paper are illustrated in Fig. 3A. The antibacterial activities of *S. aureus*, a gram-positive bacterium, and *E. coli*, a gram-negative bacterium, were tested using the agar diffusion method. As portrayed in Fig. 3A, the base paper and PP paper showed no bacteriostatic effect on *E. coli* and *S. aureus*, and the bacteriostatic circle was 0 mm. On the contrary, when TTO microcapsules were added to the paper, the inhibition zones of PP/TTO paper on *E. coli* and *S. aureus* reached 17.49 mm and 22.75 mm, respectively, and the effect on *S. aureus* was better. The experimental results of inhibition rate and zone methods were identical, but, as can be seen from Fig. 3B, the base paper and PP paper showed some inhibition effects on bacterial growth. We believe that the rough surface of the paper itself might have carried some microorganisms(Gao et al., 2023), which yielded a lower OD value compared with the control. The bacteriostatic rates of PP/TTO paper against *E. coli* and *S. aureus* reached 55.77% and 56.14%, respectively. The antibacterial rate of microcapsule (cinnamaldehyde)/cellulose nanofiber membrane to *E. coli* reached 67.01% at 6 h and pH 4.0(Wu et al., 2024). The results further verified that the bacteriostatic effect of PP/TTO paper against *S. aureus* was stronger than that against *E. coli*, which is also consistent with the bacteriostatic effect of TTO microcapsules.

#### 3.6.2. Ultrastructure of the antibacterial food packaging paper

As can be seen from the SEM image in Fig. 3C, after adding the PP/

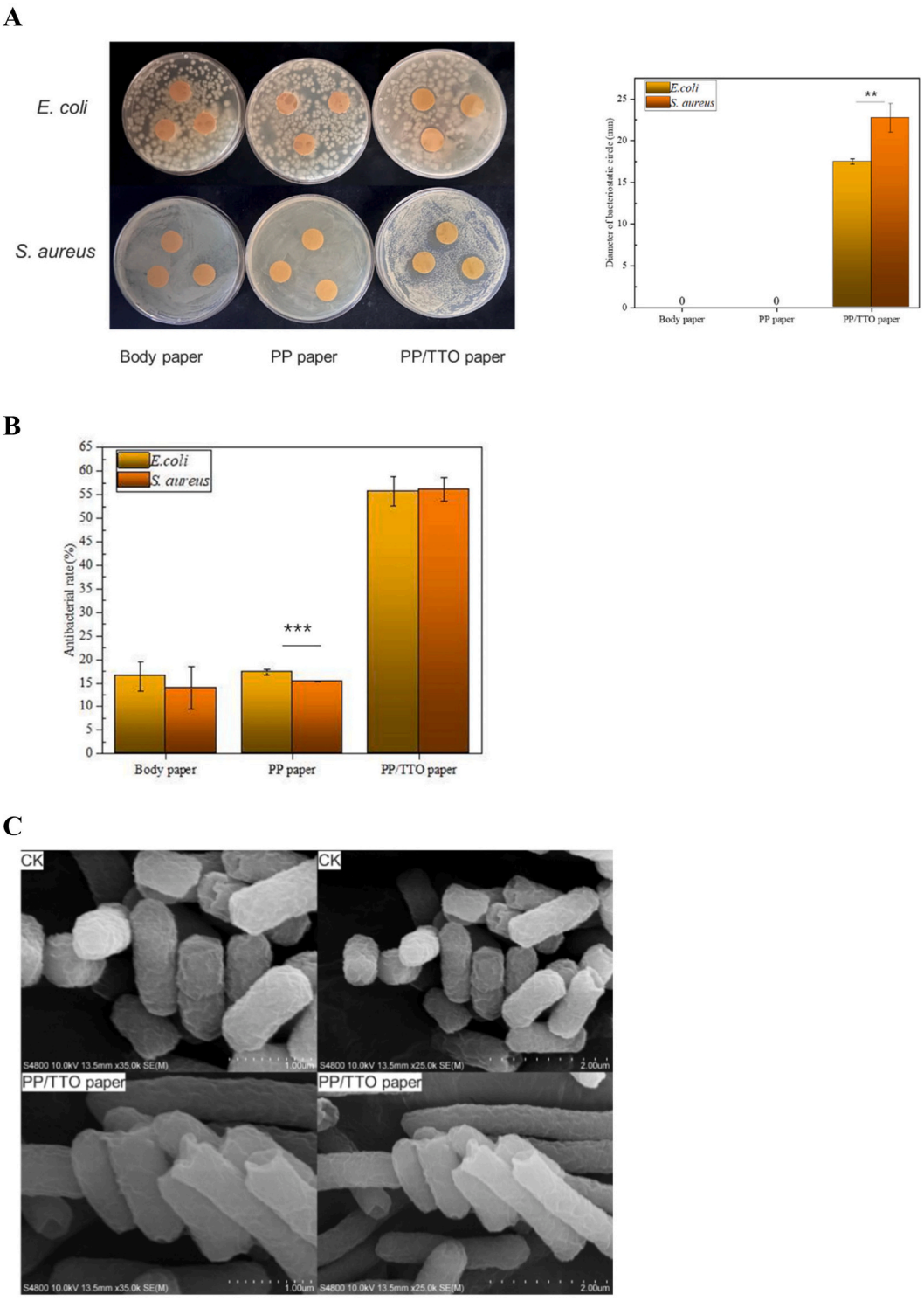


**Fig. 3.** Antibacterial circle diagram of antibacterial food packaging paper (A). The antibacterial rate chart of antibacterial food packaging paper (B). Observation of the antibacterial ultrastructure of antibacterial food packaging paper (Fig. C shows that *Escherichia coli* D is *Staphylococcus aureus*). The magnification is 35,000 times and 25,000 times, respectively.

TTO paper, the ultrastructure of the two strains changed. When compared with the non-antibacterial food packaging paper, *E. coli* became slender from the original short rod, and its port was broken. For *S. aureus*, its circular shape was not seen, and compared with the original strain, the bacteria shrank, deformed, festered, and reunited and the cell membrane was no longer complete. TTO induces bacteriostasis by irreversibly destroying the plasma membrane. In addition, the cell membrane is damaged, which results in the loss of protein, nucleic acid, and other cellular components, leading to cell death. This finding is consistent with current and previous research results(Mao et al., 2023; Meenu, Padhan, Patel, Patel, & Xu, 2023; Wang et al., 2023), that is, TTO has superior antibacterial effects on gram-positive bacteria. Collectively, these results establish the antibacterial properties of the paper containing TTO.

D

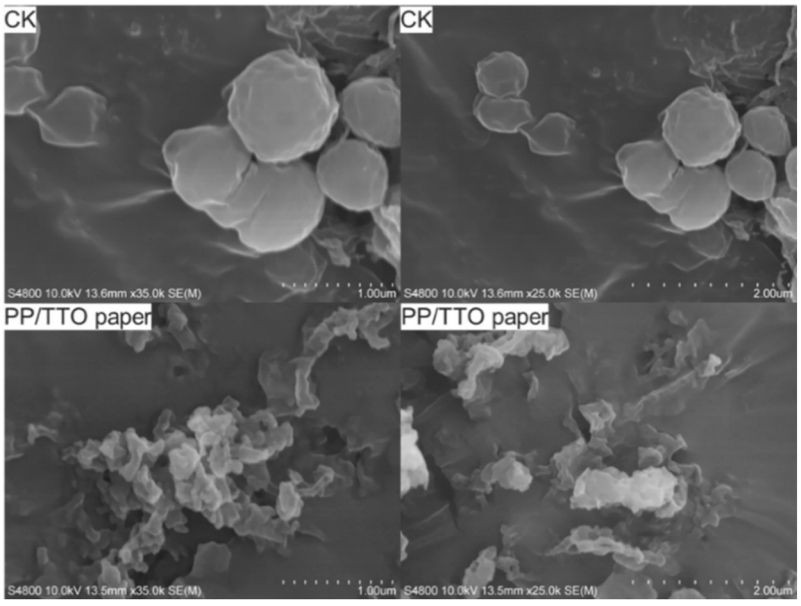


**Fig. 3.** (*continued*).

### *3.7. Characterization and measurement of the antibacterial packaging paper*

#### *3.7.1. Scanning electron microscopy of the antibacterial packaging paper*

To explore the influence of PP and PP/TTO coating on antibacterial packaging paper, SEM was used to examine the surface morphologies of different papers. Fig. 4 shows the SEM images of different papers, namely base paper, PP paper, and PP/TTO paper. As presented in the figure, the surface and cross-section of the base paper were made up of a plurality of staggered plant fibers, and the structure was loose and porous. The surface fiber structure of the PP paper had obviously disappeared, but large particles were present on the surface locally. In the cross-section, the original fibrous pores were reduced and the bonding state appeared. When PP/TTO microcapsules were added to the coating, a smooth and flat whole structure was formed on the surface, the porosity of the surface was very small, and there were no gaps or pores. Half of the cross-section was the coating itself, and the other half was the bonded fiber structure. When the paper coating was covered, because it formed a dense film on the paper surface, its pores were considerably reduced. The fiber gaps of cellulose in the base paper were easily absorbed by liquid water or oil via capillary action on the surface of the base paper. Hence, a part of the coating solution was absorbed by the pores(Priyadarshi, Riahi, & Rhim, 2024). Therefore, PP paper and PP/TTO paper cross-section fibers were in a bonding state, which indicates the uniform distribution of the coating solution. The smooth surface of PP paper and PP/TTO paper and the bonding state of the cross-section indicate that the coating evenly filled the space between cellulose fibers, which ensured better waterproof performance compared with the base paper(Harikrishnan et al., 2023). These findings allude that the paper becomes smoother upon adding the PP/TTO coating.

#### *3.7.2. X-ray diffraction analysis of the antibacterial packaging paper*

The analysis results of base paper, PP paper, and PP/TTO paper are depicted in Fig. 5A. The diffraction peaks of the base paper were observed at 15.1°, 20.4°, 22.6°, 26.5°, 29.4°, and 36.1°, which agrees with the results of(Jiang et al., 2023). The characteristic peaks of the base paper itself were mainly seen, and there were obvious diffraction peaks at 2θ = 15.1°, 22.6°, and 36.1°, which corresponded to the fact that the crystal planes (110), (200), and (004) belonged to cellulose I. Moreover, there were characteristic peaks at 2θ = 20.4° and 22.6°, which corresponded to crystal planes ((1−10) and (110)) belonged to cellulose II type(Profili et al., 2020). 26.5°, 29.4°, and some miscellaneous peaks were extra peaks caused by calcium carbonate additives(Lai et al., 2022) (usually added to the paper to improve its opacity, printability, brightness, and fiber coverage). The diffraction patterns of PP paper and PP/TTO paper were consistent with those of the original paper. Hence, the cellulose crystal structure of the paper did not change, and the treatment method had little influence on the fiber crystal structure. However, in PP paper and PP/TTO paper, the intensity of the characteristic absorption peak weakened gradually, and the crystallinity of cellulose decreased gradually, which could be ascribed to the fact that when the paper coating is covered, the coating forms a dense film on the paper surface. Therefore, liquid water or oil passes easily through the gaps of cellulose fibers and is absorbed by the pores on the surface of the base paper via capillary action(Harikrishnan et al., 2023). Furthermore, owing to the covering of the coating solution, the degree of cellulose dissolution increases, and certain cellulose crystallization areas are destroyed (Li, Liu, Tang, Zhang, & Gao, 2023).

#### *3.7.3. Fourier transform infrared spectrum of the antibacterial packaging paper*

Fig. 5B shows that the absorption peaks of pullulan at 3355 $cm^{-1}$ and 2900 $cm^{-1}$ were the stretching vibration of O—H and C—H, respectively, and the characteristic peaks at 1650 $cm^{-1}$, 1125 $cm^{-1}$, and 1022 $cm^{-1}$ were the stretching vibration peaks of O-C-O, C-O-C, and C—O, respectively(Sugumaran, Jothi, & Ponnusami, 2014). The peak at approximately 845 $cm^{-1}$ was due to the α-configuration of α-D-glucopyranoside(D. Wang, Ju, Zhou, & Wei, 2014). The characteristic peaks at 755 $cm^{-1}$ and 920 $cm^{-1}$ corresponded to the α-(1–4) and (1–6)-D-glycosidic bonds(Xiao et al., 2024), respectively. Both pullulan powder and pure pullulan paper exhibited the characteristic peaks of pullulan. After adding TTO microcapsules, PP/TTO paper also mainly displayed the characteristic absorption peaks of pullulan, of which the absorption peaks of TTO microcapsules were seen at 2919 $cm^{-1}$ and 1371 $cm^{-1}$. The characteristic peaks of pullulan at 3355 $cm^{-1}$, 2900 $cm^{-1}$, 1650 $cm^{-1}$, 1125 $cm^{-1}$, 1022 $cm^{-1}$, 845 $cm^{-1}$, 755 $cm^{-1}$, and 920 $cm^{-1}$ shifted slightly, which signifies that pullulan solution and TTO microcapsules formed a coating via hydrogen bonds(Zhou et al., 2023).

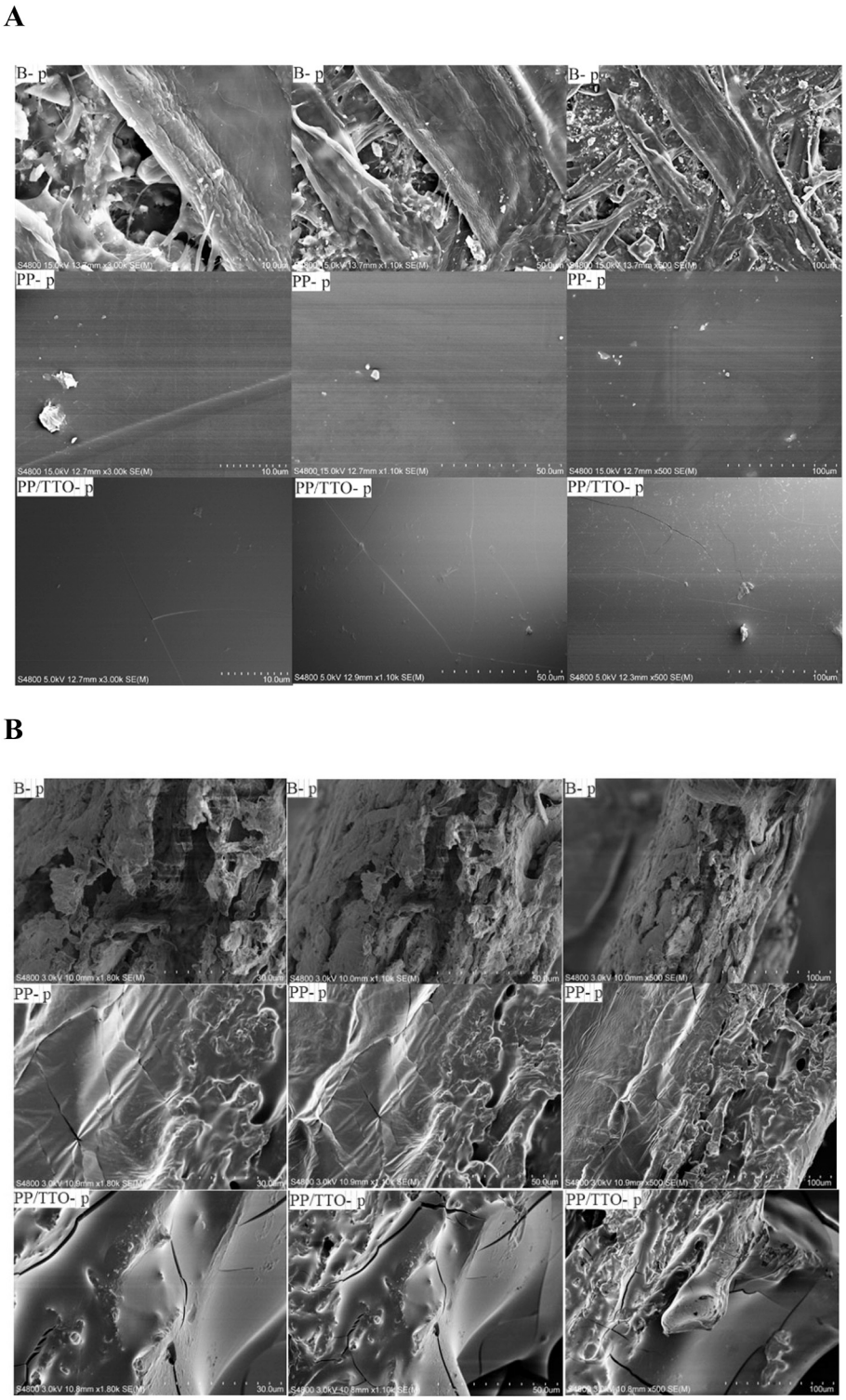


**Fig. 4.** Scanning electron microscopic observation of antibacterial wrapping paper. (A) The paper surface; the magnification of B-p, PP-p, and PP/TTO-p are 1800 times, 1100 times, and 500 times, respectively; (B) the paper section; the magnification of B-p, PP-p, and PP/TTO-p are 1800 times, 1100 times, and 500 times, respectively.

*3.7.4. Thermal stability of the antibacterial packaging paper*

The thermal stability of the food packaging paper was characterized using TGA and DTG tests. Fig. 5C shows that the thermal stabilities of the three types of paper were very similar because the raw materials from which they were prepared were the same. The base paper, PP paper, and PP/TTO paper demonstrated two weight loss intervals. The first weight loss interval was between 50 °C and 85 °C, which corresponded to evaporation and the loss of water and solvent, and the second weight loss interval occurred between 300 °C and 350 °C. Finally, the residual rates of base paper, PP paper, and PP/TTO paper were 25.16%, 20.41%, and 13.32%, respectively. After adding PP and TTO, the thermal stability of the paper decreased to a certain extent. The lower the crystallinity of the polymer, the easier the thermal degradation(Fei, Huang, Yin, Xu, & Zhang, 2015). However, the maximum degradation

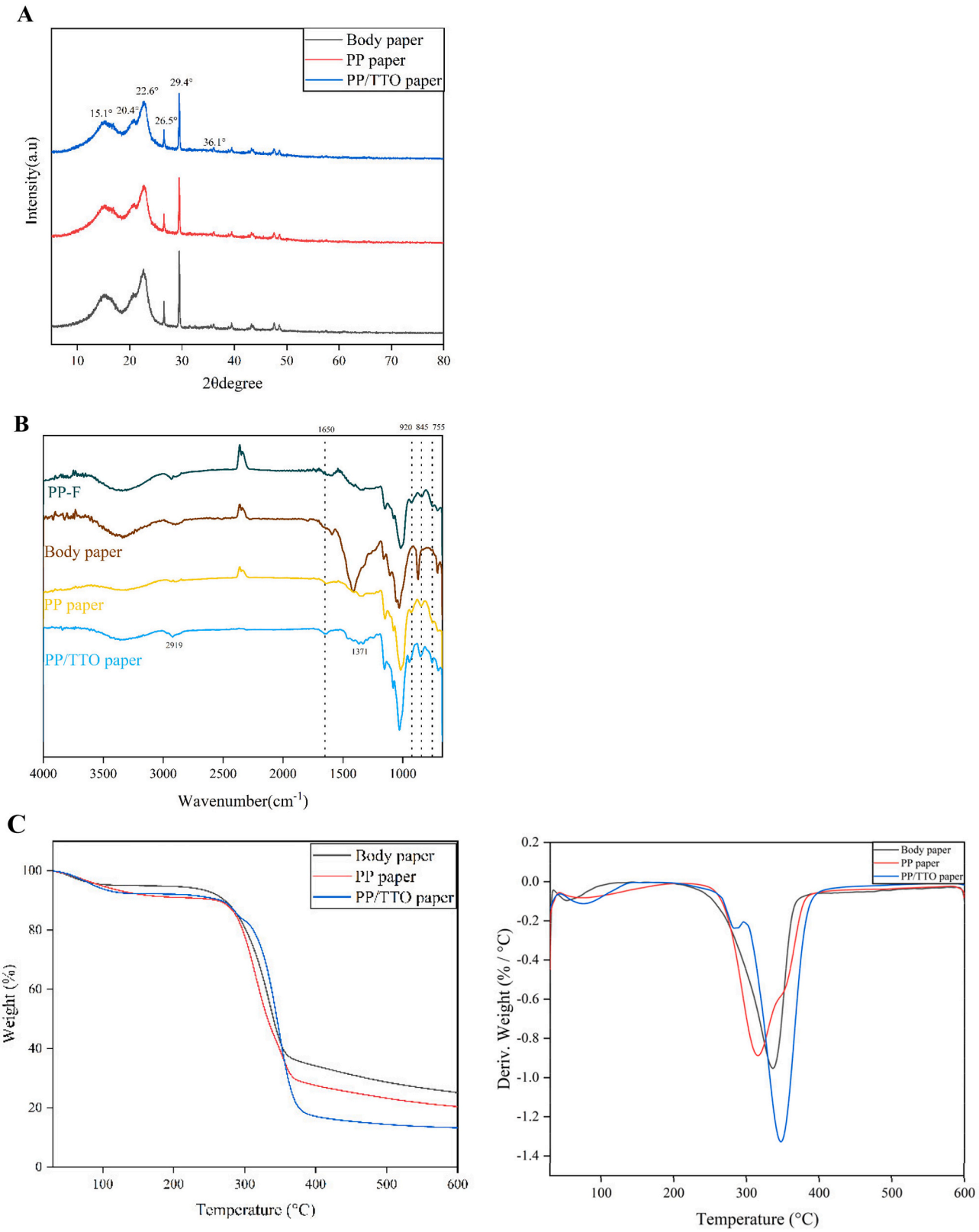


**Fig. 5.** X-ray diffraction (XRD) diagram of antibacterial packaging paper (A). The Fourier infrared spectrum of antibacterial packaging paper (B). TGA and DTG analysis chart of antibacterial food packaging paper (C).

temperature moved to the right when TTO was added to the packaging paper. The temperature required to attain the maximum thermal degradation rate was the highest (347.38 °C) for PP/TTO paper, and its degradation rate was also the greatest. Yang et al. (2024) added cinnamon essential oil emulsion (15%) to chitosan film. When compared with pure chitosan film, the temperature required for its maximum thermal degradation rate increased from 260 °C to 280 °C. When cinnamon essential oil emulsion was added to composite films, the weight losses of all composite films were greater than those of pure gelatin films, and the maximum degradation temperature was shifted to the right when the concentration of cinnamon essential oil emulsion reached 12%(Li et al., 2024). The paper prepared in this study did not undergo thermal decomposition below 288 °C. Hence, its thermal stability is sufficient to meet the industrial requirements(Fei et al., 2015).

### *3.7.5. Atomic force microscopy of the antibacterial packaging paper*

AFM was used to analyze the surface morphology of the antibacterial packaging paper with coating. As presented in Fig. 6, when the AFM scanning range was 10 μm, the surface of the base paper was rough, and its surface roughness was 28.5 nm (Rq) and 22.1 nm (Ra). On the contrary, the surface roughness of PP paper was 49.4 nm (Rq) and 41.7 nm (Ra), and the surface of PP/TTO paper was smooth. The surface roughness of PP/TTO paper was 7.16 nm (Rq) and 5.61 nm (Ra), which agrees with the results of SEM; the pure SA film prepared by Mao et al. (2023) was very smooth, with an average roughness (Ra) and root mean square roughness (Rq) of 5.70 nm and 4.52 nm, respectively. However, the higher roughness of PP paper could be attributed to the presence of large particles on its surface, which contribute to the roughness. For instance, with regard to local sedimentation and agglomeration, the values of Ra and Rq increased from 12.4 nm and 9.9 nm to 85.0 nm and 69.8 nm, respectively, for the materials prepared by Mao et al. (2023). The PP/TTO paper had the lowest surface roughness and was the smoothest of all.

## 4. Conclusion

In this work, with HP-β-CD as the wall material and TTO as the core material, TTO microcapsules were prepared using the saturated aqueous solution method, and antibacterial food packaging paper was prepared using the coating method. The morphology, structure, and crystallinity of TTO microcapsules and antibacterial food packaging paper were observed using SEM, FT-IR, and X-ray diffraction, and the roughness of the antibacterial food packaging paper was examined using AFM. The findings signified that the TTO microcapsules were granular and irregular and that the bioactive compound interacted with HP-β-CD via hydrogen bonds. The crystal configuration of TTO microcapsules did not change significantly and a new phase was generated, which displayed good temperature stability. The TTO microcapsules and the antibacterial food packaging paper prepared using them exhibited good antibacterial properties against *S. aureus* and *E. coli*. The coating was mainly formed via hydrogen bonds, and at the same time, the pores of the paper fibers were filled, which made the paper smooth and compact and reduced its roughness. The cellulose crystal structure of the paper had not changed, and the treatment method had little influence on the crystal structure of the fibers. Based on the results, the TTO microcapsule packaging paper can be used for preparing environment-friendly, smooth packaging materials with antibacterial properties. These materials hold enormous application potential in the food packaging industry. However, in this study, we did not apply plastic wrapping to real fruits and vegetables. In the future, it can be applied to fruits and vegetables to examine whether plastic wrap can regulate the quality of fruits and vegetables in addition to bacteriostasis.

## CRediT authorship contribution statement

**Lin Zhu:** Writing – review & editing, Writing – original draft, Software, Investigation, Conceptualization. **Yijun Liu:** Methodology. **Jiameng Liu:** Visualization. **Xunxia Qiu:** Writing – review & editing. **Lijing Lin:** Funding acquisition.

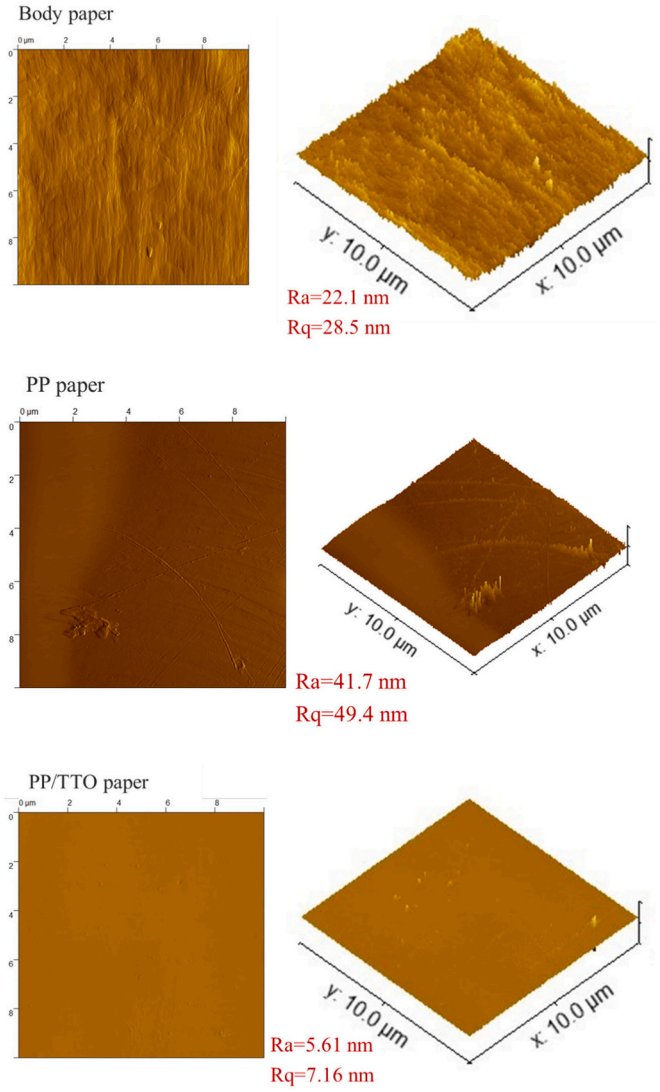


**Fig. 6.** Atomic force microscope height map and the three-dimensional map of antibacterial packaging paper.

## Declaration of competing interest

The authors declare that they have no known competing financial interests or personal relationships that could have appeared to influence the work reported in this paper.

## Data availability

The data that has been used is confidential.

## Acknowledgments

This study was funded by “High-level talents of Hainan Natural Science Foundation (321RC634)”, “Central Public-interest Scientific Institution Basal Research Fund (NO.1630122024011)”, “Hainan Key Laboratory of Storage & Processing of Fruits and Vegetables (HNGS202303, HNGS202301 and HNGS202302)”, “Central Public-interest Scientific Institution Basal Research Fund (NO.

1630062022006)", "Central Public-interest Scientific Institution Basal Research Fund (NO.1630122024006)".

## References


Ahmad, M., Qureshi, S., Maqsood, S., Gani, A., & Masoodi, F. A. (2017). Micro-encapsulation of folic acid using horse chestnut starch and β-cyclodextrin: Microcapsule characterization, release behavior & antioxidant potential during GI tract conditions. *Food Hydrocolloids, 66*, 154–160. https://doi.org/10.1016/j.foodhyd.2016.11.012

Andrade, R. A. M. D. S., Da Silva, D. C., Souza, M. M. B. D., De Oliveira, R. L., Maciel, M. I. S., Porto, A. L. F., … Porto, T. S. (2023). Microencapsulation of phenolic compounds from cashew apple (Anacardium occidentale L.) agro-food waste: Physicochemical characterization, antioxidant activity, biodisponibility and stability. *Food Chemistry Advances, 3*. https://doi.org/10.1016/j.focha.2023.100364. Article 100364.

Cao, C. A., Wei, D. M., Xu, L., Hu, J. W., Qi, J., & Zhou, Y. B. (2021). Characterization of tea tree essential oil and large-ring cyclodextrins (CD<sub>9</sub>-CD<sub>22</sub>) inclusion complex and evaluation of its thermal stability and volatility. *Journal of the Science of Food and Agriculture, 101*(7), 2877–2883. https://doi.org/10.1002/jsfa.10919

Chu, Y., Popovich, C., & Wang, Y. (2023). Heat sealable regenerated cellulose films enabled by zein coating for sustainable food packaging. *Composites Part C: Open Access, 12*. https://doi.org/10.1016/j.jcomc.2023.100390. Article 100390.

Cui, H., Bai, M., & Lin, L. (2018). Plasma-treated poly(ethylene oxide) nanofibers containing tea tree oil/beta-cyclodextrin inclusion complex for antibacterial packaging. *Carbohydrate Polymers, 179*, 360–369. https://doi.org/10.1016/j.carbpol.2017.10.011

Du, Y.-Z., Xu, J.-G., Wang, L., Yuan, H., & Hu, F.-Q. (2009). Preparation and characteristics of hydroxypropyl-β-cyclodextrin polymeric nanocapsules loading nimodipine. *European Polymer Journal, 45*(5), 1397–1402. https://doi.org/10.1016/j.eurpolymj.2009.01.031

Emadzadeh, B., Ghorani, B., Naji-Tabasi, S., Charpashlo, E., & Molaveisi, M. (2021). Fate of β-cyclodextrin-sugar beet pectin microcapsules containing garlic essential oil in an acidic food beverage. *Food Bioscience, 42*. https://doi.org/10.1016/j.fbio.2021.101029. Article 101029.

Fei, Z., Huang, S., Yin, J., Xu, F., & Zhang, Y. (2015). Preparation and characterization of bio-based degradable plastic films composed of cellulose acetate and starch acetate. *Journal of Polymers and the Environment, 23*(3), 383–391. https://doi.org/10.1007/s10924-015-0711-1

Gao, C., Chen, P., Ma, Y., Sun, L., Yan, Y., Ding, Y., & Sun, L. (2023). Multifunctional polylactic acid biocomposite film for active food packaging with UV resistance, antioxidant and antibacterial properties. *International Journal of Biological Macromolecules, 253*. https://doi.org/10.1016/j.ijbiomac.2023.126494. Article 126494.

Gao, T., Yan, L., Yu, Q., Lyu, Y., Dong, W., Chen, M., & Shi, D. (2024). High transparency, water vapor barrier and antibacterial properties of chitosan/carboxymethyl glucan/poly(vinyl alcohol)/nanoparticles encapsulating citral composite film for fruit packaging. *International Journal of Biological Macromolecules, 261*. https://doi.org/10.1016/j.ijbiomac.2024.129755. Article 129755.

Guan, Y., Zhang, J., Zhang, J., Song, W., Shi, J., Huang, X., & Zou, X. (2024). Preparation of active film based on cinnamon essential oil into β-cyclodextrin with high hydrophobic and its preservation for griskin. *Food Control, 160*. https://doi.org/10.1016/j.foodcont.2024.110344. Article 110344.

Ham-Pichavant, F., Sèbe, G., Pardon, P., & Coma, V. (2005). Fat resistance properties of chitosan-based paper packaging for food applications. *Carbohydrate Polymers, 61*(3), 259–265. https://doi.org/10.1016/j.carbpol.2005.01.020

Harikrishnan, M. P., Thampi, A., Lal, A. M. N., Warrier, A. S., Basil, M., & Kothakota, A. (2023). Effect of chitosan-based bio coating on mechanical, structural and physical characteristics of microfiber based paper packaging: An alternative to wood pulp/plastic packaging. *International Journal of Biological Macromolecules, 253*. https://doi.org/10.1016/j.ijbiomac.2023.126888. Article 126888.

Hu, D., Xu, Y., Gao, C., Meng, L., Feng, X., Wang, Z., & Tang, X. (2024). Preparation and characterization of starch/PBAT film containing hydroxypropyl-β-cyclodextrin/ethyl lauroyl arginate/cinnamon essential oil microcapsules and its application in the preservation of strawberry. *International Journal of Biological Macromolecules, 259*. https://doi.org/10.1016/j.ijbiomac.2024.129204. Article 129204.

Hu, G., Luo, F., Han, J., Li, J., Zhou, C., Yang, C., & Hu, Y. (2023). EGCG/HP-β-CD inclusion complexes integrated into PCL/chitosan oligosaccharide nanofiber membranes developed by ELS for fruit packaging. *Food Hydrocolloids, 144*. https://doi.org/10.1016/j.foodhyd.2023.108992. Article 108992.

Hu, R., Wang, S., Feng, L., Jiang, W., Wu, P., Liu, Y., & Zhou, X. (2023). Alleviation of hypoxia stress induced oxidative damage, endoplasmic reticulum stress (ERS) and autophagy in grass carp (Ctenopharyngodon idellu) by TTO (Melaleuca alternifolia essential oil). *Aquaculture, 564*. https://doi.org/10.1016/j.aquaculture.2022.739073. Article 739073.

Huang, J., Pu, J., Yang, Z., Zhang, S., Zhang, Z., Lu, Q., & Hu, B. (2024). Development of a Syzygium aromaticum, L. essential oil/hydroxypropyl-β-cyclodextrin inclusion complex: Preparation, characterization, and evaluation. *Industrial Crops and Products, 214*. https://doi.org/10.1016/j.indcrop.2024.118500. Article 118500.

Huang, J., Zhang, S., Liu, D., Feng, X., Wang, Q., An, S., & Chu, L. (2024). Preparation and characterization of astaxanthin-loaded microcapsules stabilized by lecithin-chitosan-alginate interfaces with layer-by-layer assembly method. *International Journal of Biological Macromolecules, 268*. https://doi.org/10.1016/j.ijbiomac.2024.131909. Article 131909.

Inthamat, P., Karbowiak, T., Tongdeesoontorn, W., & Siripatrawan, U. (2024). Biodegradable active coating from chitosan/astaxanthin crosslinked with genipin to improve water resistance, moisture and oxygen barrier and mechanical properties of Kraft paper. *International Journal of Biological Macromolecules, 254*. https://doi.org/10.1016/j.ijbiomac.2023.127816. Article 127816.

Jayakumar, A., Radoor, S., Kim, J. T., Rhim, J. W., Nandi, D., Parameswaranpillai, J., & Siengchin, S. (2022). Recent innovations in bionanocomposites-based food packaging films – A comprehensive review. *Food Packaging and Shelf Life, 33*. https://doi.org/10.1016/j.fpsl.2022.100877. Article 100877.

Jiang, X., Liu, S., Yang, Q., Sun, D., Yang, K., Yuan, Z., & Du, J. (2023). Facile fabrication of highly flame-retardant superhydrophobic coatings on Kraft paper via a simple and efficient method. *Colloid and Interface Science Communications, 57*. https://doi.org/10.1016/j.colcom.2023.100755. Article 100755.

Karami-Eshkaftaki, Z., Saei-Dehkordi, S., Albadi, J., Moradi, M., & Saei-Dehkordi, S. S. (2024). Coated composite paper with nano-chitosan/cinnamon essential oil-nanoemulsion containing grafted CNC@ZnO nanohybrid; synthesis, characterization and inhibitory activity on Escherichia coli biofilm developed on grey zucchini. *International Journal of Biological Macromolecules, 258*. https://doi.org/10.1016/j.ijbiomac.2023.128981. Article 128981.

Khwaldia, K. (2010). Water vapor barrier and mechanical properties of paper-sodium CASEINATE and paper-sodium CASEINATE-paraffin wax films. *Journal of Food Biochemistry, 34*(5), 998–1013. https://doi.org/10.1111/j.1745-4514.2010.00345.x

Kızılyıldırım, S., Kandemir, T., Kendir, G., Muhammed, M. T., Köroğlu, A., Köksal, F., & Ozogul, F. (2024). The antibacterial effect mechanisms of Laurus nobilis extracts on carbapenem-resistant Acinetobacter baumanii isolates. *Food Bioscience, 59*. https://doi.org/10.1016/j.fbio.2024.104011. Article 104011.

Kong, P., Abe, J. P., Masuo, S., & Enomae, T. (2023). Preparation and characterization of tea tree oil-β-cyclodextrin microcapsules with super-high encapsulation efficiency. *Journal of Bioresources and Bioproducts, 8*(3), 224–234. https://doi.org/10.1016/j.jobab.2023.03.004

Kunam, P. K., Anushikha, & Gaikwad, K. K. (2023). Water resistant paper based on natural rubber latex from Hevea brasiliensis and butyl stearate hydrophobic coating for packaging applications. *Industrial Crops and Products, 205*. https://doi.org/10.1016/j.indcrop.2023.117480. Article 117480.

Lai, C. Q., Lim, G. Y., Tai, K. J., Lim, K. J. D., Yu, L., Kanaujia, P. K., & Seetoh, P. I. (2022). Exceptional energy absorption characteristics and compressive resilience of functional carbon foams scalably and sustainably derived from additively manufactured Kraft paper. *Additive Manufacturing, 58*. https://doi.org/10.1016/j.addma.2022.102992. Article 102992.

Li, B., Liu, G., Tang, X., Zhang, H., & Gao, X. (2023). Facile preparation of all cellulose composite with excellent mechanical and antibacterial properties via partial dissolution of corn-stalk biomass. *International Journal of Biological Macromolecules, 228*, 89–98. https://doi.org/10.1016/j.ijbiomac.2022.12.212

Li, D., Li, E.-J., Li, L., Li, B., Jia, S., Xie, Y., & Zhong, C. (2024). Effect of TEMPO-oxidized bacterial cellulose nanofibers stabilized Pickering emulsion of cinnamon essential oil on structure and properties of gelatin composite films. *International Journal of Biological Macromolecules, 264*. https://doi.org/10.1016/j.ijbiomac.2024.130344. Article 130344.

Li, J., Hou, X., Jiang, L., Xia, D., Chen, A., Li, S., & Zhang, Z. (2022). Optimization and characterization of Sichuan pepper (Zanthoxylum bungeanum maxim) resin microcapsule encapsulated with β-cyclodextrin. *LWT, 171*. https://doi.org/10.1016/j.lwt.2022.114120. Article 114120.

Lian, R., Cao, J., Jiang, X., & Rogachev, A. V. (2021). Physicochemical, antibacterial properties and cytocompatibility of starch/chitosan films incorporated with zinc oxide nanoparticles. *Materials Today Communications, 27*. https://doi.org/10.1016/j.mtcomm.2021.102265. Article 102265.

Mao, S., Ren, Y., Wei, C., Chen, S., Ye, X., & Jinhu, T. (2023). Development of novel EGCG/Fe loaded sodium alginate-based packaging films with antibacterial and slow-release properties. *Food Hydrocolloids, 145*. https://doi.org/10.1016/j.foodhyd.2023.109032. Article 109032.

Medeleanu, M. L., Fărcaș, A. C., Coman, C., Leopold, L., Diaconeasa, Z., & Socaci, S. A. (2023). Citrus essential oils – Based nano-emulsions: Functional properties and potential applications. *Food Chemistry: X, 20*. https://doi.org/10.1016/j.fochx.2023.100960. Article 100960.

Meenu, M., Padhan, B., Patel, M., Patel, R., & Xu, B. (2023). Antibacterial activity of essential oils from different parts of plants against Salmonella and Listeria spp. *Food Chemistry, 404*. https://doi.org/10.1016/j.foodchem.2022.134723. Article 134723.

Munhuweyi, K., Caleb, O. J., van Reenen, A. J., & Opara, U. L. (2018). Physical and antifungal properties of β-cyclodextrin microcapsules and nanofibre films containing cinnamon and oregano essential oils. *LWT, 87*, 413–422. https://doi.org/10.1016/j.lwt.2017.09.012

Pinto, E. P., Menezes, R. P., Pires, M. A., Zamora, R. R. M., Araújo, R. S., Souza, T. M., & d.. (2023). Comparing the nanoscale topography and interface properties of chitosan films containing free and nano-encapsulated copaiba essential oil: An atomic force microscopy (AFM) and fractal geometry study. *Materials Today Communications, 35*. https://doi.org/10.1016/j.mtcomm.2023.105765. Article 105765.

Priyadarshi, R., Riahi, Z., & Rhim, J.-W. (2024). Alginate-coated functional wrapping paper incorporated with sulfur quantum dots and grapefruit seed extract for preservation of potato hash browns. *Sustainable. Materials and Technologies, 40*. https://doi.org/10.1016/j.susmat.2024.e00942. Article e00942.

Profili, J., Asadollahi, S., Vinchon, P., Dorris, A., Beck, S., Sarkassian, A., & Stafford, L. (2020). Recent progress on organosilicon coatings deposited on bleached unrefined Kraft paper by non-thermal plasma process at atmospheric pressure. *Progress in Organic Coatings, 147*. https://doi.org/10.1016/j.porgcoat.2020.105865. Article 105865.

Qiang, Y., Wei, H., Huang, B., Chi, H., & Fu, J. (2024). Inclusion complex of turmeric essential oil with hydroxypropyl-β-cyclodextrin: Preparation, characterization and release kinetics. *Current Research in Food Science, 8*. https://doi.org/10.1016/j.crfs.2023.100668. Article 100668.

Sugumaran, K. R., Jothi, P., & Ponnusami, V. (2014). Bioconversion of industrial solid waste—Cassava bagasse for pullulan production in solid state fermentation. *Carbohydrate Polymers, 99*, 22–30. https://doi.org/10.1016/j.carbpol.2013.08.039

Sun, X., Zhu, J., Liu, C., Wang, D., & Wang, C.-Y. (2022). Fabrication of fucoxanthin/2-hydroxypropyl-β-cyclodextrin inclusion complex assisted by ultrasound procedure to enhance aqueous solubility, stability and antitumor effect of fucoxanthin. *Ultrasonics Sonochemistry, 90*. https://doi.org/10.1016/j.ultsonch.2022.106215. Article 106215.

Wang, C., Yan, T., Yan, T., & Wang, Z. (2023). Fabrication of hesperetin/hydroxypropyl-β-cyclodextrin complex nanoparticles for enhancement of bioactivity using supercritical antisolvent technology. *Journal of Molecular Structure, 1279*. https://doi.org/10.1016/j.molstruc.2023.134947. article 134947.

Wang, D., Ju, X., Zhou, D., & Wei, G. (2014). Efficient production of pullulan using rice hull hydrolysate by adaptive laboratory evolution of Aureobasidium pullulans. *Bioresource Technology, 164*, 12–19. https://doi.org/10.1016/j.biortech.2014.04.036

Wang, X., Xuan, S., Ding, K., Jin, P., Zheng, Y., & Wu, Z. (2024). Photothermal controlled antibacterial Ta4C3Tx-AgNPs/nanocellulose bioplastic food packaging. *Food Chemistry, 448*. https://doi.org/10.1016/j.foodchem.2024.139126. Article 139126.

Wang, Y., Cheng, M., Yan, X., Zhao, P., Wang, K., Wang, Y., & Wang, J. (2023). Preparation and characterization of an active packaging film loaded with tea tree oil-hydroxyapatite porous microspheres. *Industrial Crops and Products, 199*. https://doi.org/10.1016/j.indcrop.2023.116783. Article 116783.

Wen, P., Zhu, D.-H., Feng, K., Liu, F.-J., Lou, W.-Y., Li, N., & Wu, H. (2016). Fabrication of electrospun polylactic acid nanofilm incorporating cinnamon essential oil/β-cyclodextrin inclusion complex for antimicrobial packaging. *Food Chemistry, 196*, 996–1004. https://doi.org/10.1016/j.foodchem.2015.10.043

Wu, M., Xue, Z., Wang, C., Wang, T., Zou, D., Lu, P., & Song, X. (2024). Smart antibacterial nanocellulose packaging film based on pH-stimulate responsive microcapsules synthesized by Pickering emulsion template. *Carbohydrate Polymers, 323*. https://doi.org/10.1016/j.carbpol.2023.121409. Article 121409.

Xia, Y., Wang, S., Meng, F., Xu, Z., Fang, Q., Gu, Z., & Kong, F. (2024). Eco-friendly food packaging based on paper coated with a bio-based antibacterial coating composed of carbamate starch, calcium lignosulfonate, cellulose nanofibrils, and silver nanoparticles. *International Journal of Biological Macromolecules, 254*. https://doi.org/10.1016/j.ijbiomac.2023.127659. Article 127659.

Xiao, M., Tan, M., Peng, C., Jiang, F., Wu, K., Liu, N., & Yao, X. (2024). Soft and flexible polyvinyl alcohol/pullulan aerogels with fast and high water absorption capacity for facial mask substrates. *International Journal of Biological Macromolecules, 264*. https://doi.org/10.1016/j.ijbiomac.2024.130469. Article 130469.

Yang, L., Guo, Z., Li, W., Gou, Q., Han, L., & Yu, Q. (2022). The impact of lemon seeds oil microcapsules based on a bilayer macromolecule carrier on the storage of the beef jerky. *Food Packaging and Shelf Life, 32*. https://doi.org/10.1016/j.fpsl.2022.100838. Article 100838.

Yang, L., Zhou, C., Liu, Y., He, Z., Zhang, M., Wang, C., & Li, P. (2024). Enhanced mechanical properties and antibacterial activities of chitosan films through incorporating zein-gallic acid conjugate stabilized cinnamon essential oil Pickering emulsion. *International Journal of Biological Macromolecules, 258*. https://doi.org/10.1016/j.ijbiomac.2023.128933. Article 128933.

Ying, T., Jiang, C., Munir, S., Liu, R., Yin, T., You, J., & Hu, Y. (2024). Synthesis and application of gelatin-based controlled-release antibacterial films containing oregano essential oil/β-cyclodextrin microcapsules for chilling preservation of grass carp fillets. *Food Chemistry, 451*. https://doi.org/10.1016/j.foodchem.2024.139465. Article 139465.

Zhou, F., Yu, L., Liu, Y., Zeng, Z., Li, C., Fang, Z., & Liu, Y. (2023). Effect of hydroxypropyl-β-cyclodextrin and lecithin co-stabilized nanoemulsions on the konjac glucomannan/pullulan film. *International Journal of Biological Macromolecules, 235*. https://doi.org/10.1016/j.ijbiomac.2023.123802. Article 123802.

Zhu, L., Luo, H., Shi, Z.-W., Lin, C.-Q., & Chen, J. (2023). Preparation, characterization, and antibacterial effect of bio-based modified starch films. *Food Chemistry: X, 17*. https://doi.org/10.1016/j.fochx.2023.100602. Article 100602.